started from the day of the experiment and most of the doxorubicin was released by day 8. Unlike the previous result, sustained release was not detected in this drug-enriched sheet. The sheet did not retain doxorubicin after 12 days of experiments.

Biodegradation of the sheet in mice. Since deliberate release of the drug from the sheet was demonstrated *in vitro*, the biodegradability of the sheet was examined next. After implantation of the sheet into the left flank of the mice, changes in the dry-weight of the sheet were measured and recorded chronologically. The sheet degraded according to the passage of time. Degradation rapidly progressed in the initial stage and continued until day 78. The sheet was ultimately absorbed. It took more than 80 days to disappear and further changes in weight could not be determined. During the process, the doxorubicin sheet was assimilated and other than pigmentation in the adjacent area, caused

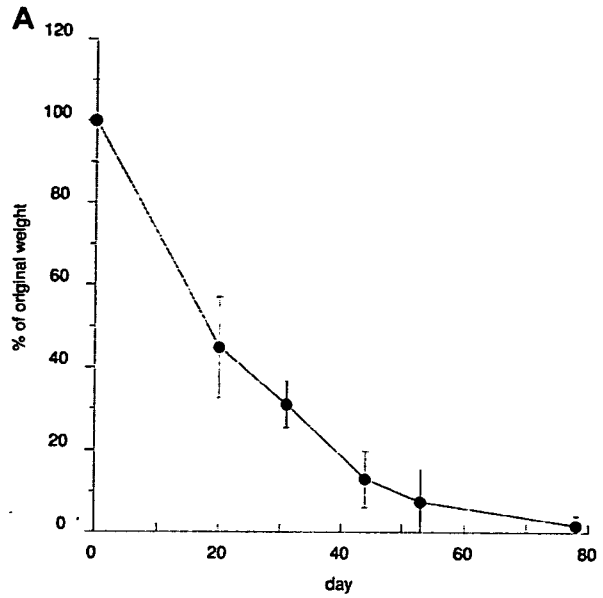

Figure 2. *Biodegradability of the sheet in vivo. A) The dry-weight of the implanted sheet was measured and biodegradability was expressed as a percentage of the original weight. The sheet degraded according to the passage of time. There was a rapid decrease in volume from the start of the experiment, followed by gradual degradation. More than 78 days were required for complete absorption. The result is expressed as the mean of five animals at each time point; bars, S.D. B) Biodegradability of the subcutaneously implanted sheet. The picture shows the sheets at 52 days after implantation. The sheet was degraded, but still visible with a change in the color of the surrounding subcutaneous tissue. Pigmentation of tissue occurred in the contact area of the sheet.*

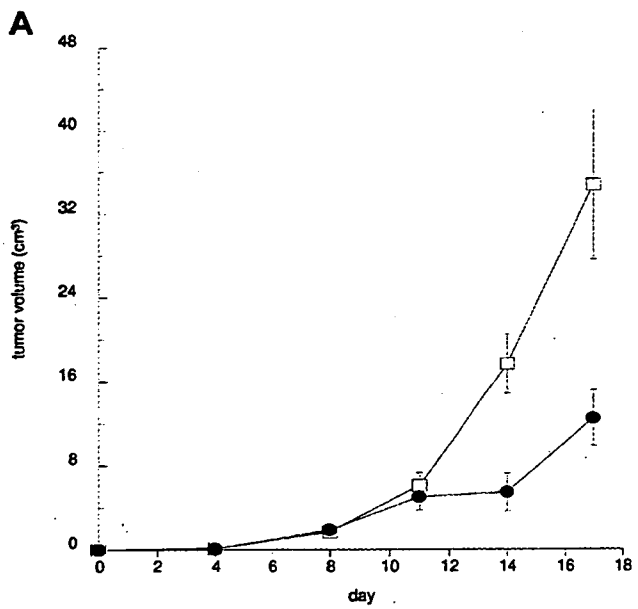

neither inflammation nor substantial necrosis in the surrounding tissue (Figure 2A, B).

Effect of the released doxorubicin on the established tumor. The slow-release character and biodegradability of the sheet enables potential application of the sheet for tumor treatment *in vivo*. In the final examination, the sheet was used for the treatment of subcutaneously implanted RT2 syngeneic malignant glioma tumor cells. After growth, the tumor was covered with a doxorubicin sheet and the subsequent growth was measured. Tumors treated with a mock sheet increased in size exponentially (Figure 3). In contrast, growth of the tumor was inhibited in rats treated with the doxorubicin sheet. On the 17th day of the experiment, the tumor volume reached more than 30 cm^3 and the rats started to die in the control group, whereas the group treated with the doxorubicin sheet exhibited a smaller tumor size. There were inter-group differences in volumes

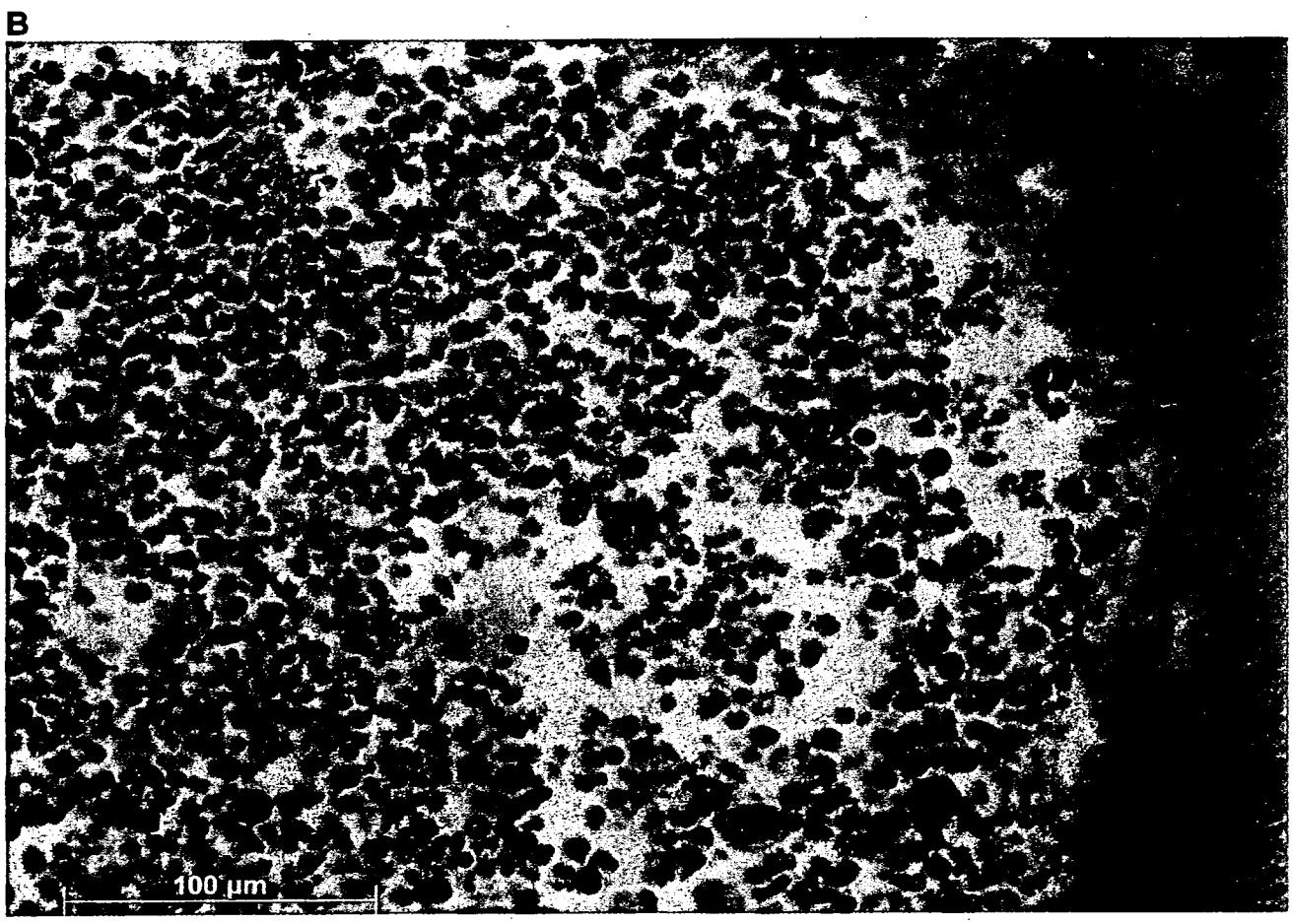

Figure 3. *Tumor growth inhibition by the sheet. A) After glioma cells were implanted, the tumor nodule was treated to the sheet. While tumors in control animals grew prosperously, treatment inhibited the expansion of the tumor. Mock sheet treatment (□); doxorubicin sheet treatment (●). There were differences on day 14 ($p=0.064$) and day 17 ($p=0.019$). The result was demonstrated as a mean of five animals in each group; bars, S.D. B) Histology of tumor cells with the sheet (on day 17, hematoxylin-eosin staining). Tumor tissue or cells (left) adjoining the sheet (right) were necrotic with erythrocytes.*

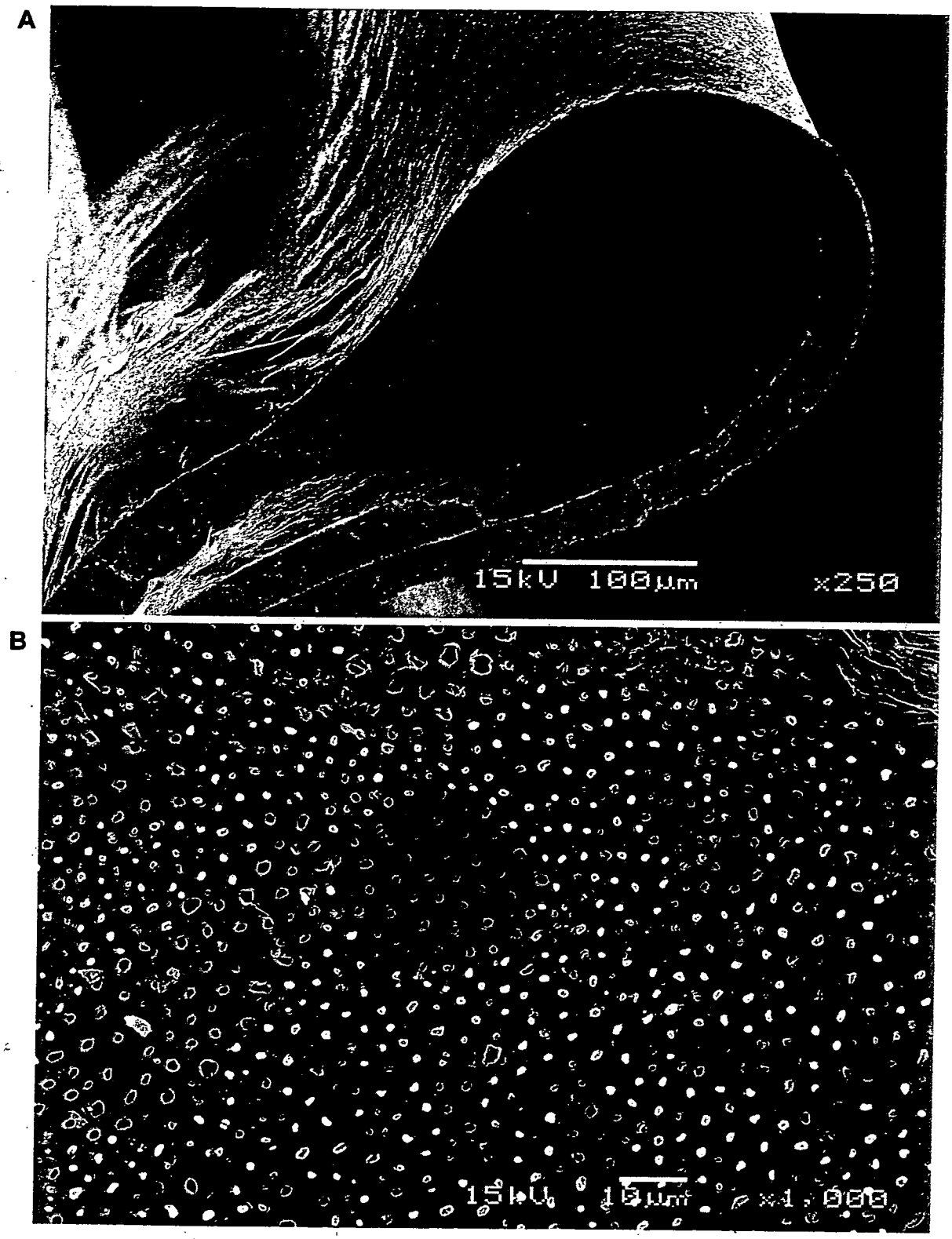

Figure 4. *Ultrastructure of doxorubicin sheet by electron microscopy. A-C) Pictures taken by scanning electron microscope, D) By transmission electron microscope. A) Overview: the sheet had a flexible texture with a thickness of 10 µm. B) Surface: the surface consisted of amorphous material with small holes. Grains of the drug resided in these small holes with a diameter of 0.5 to 3 µm. C) Vertical section (ethanol-cracked surface): after fixation, the sample was ethanol-cracked in liquid nitrogen. Cross-section disclosed the porous structure of the membrane sheet. D) Cross-section of the sheet: the drug was encircled by an amorphous electro-density substrate. Direct magnification, x15000.*

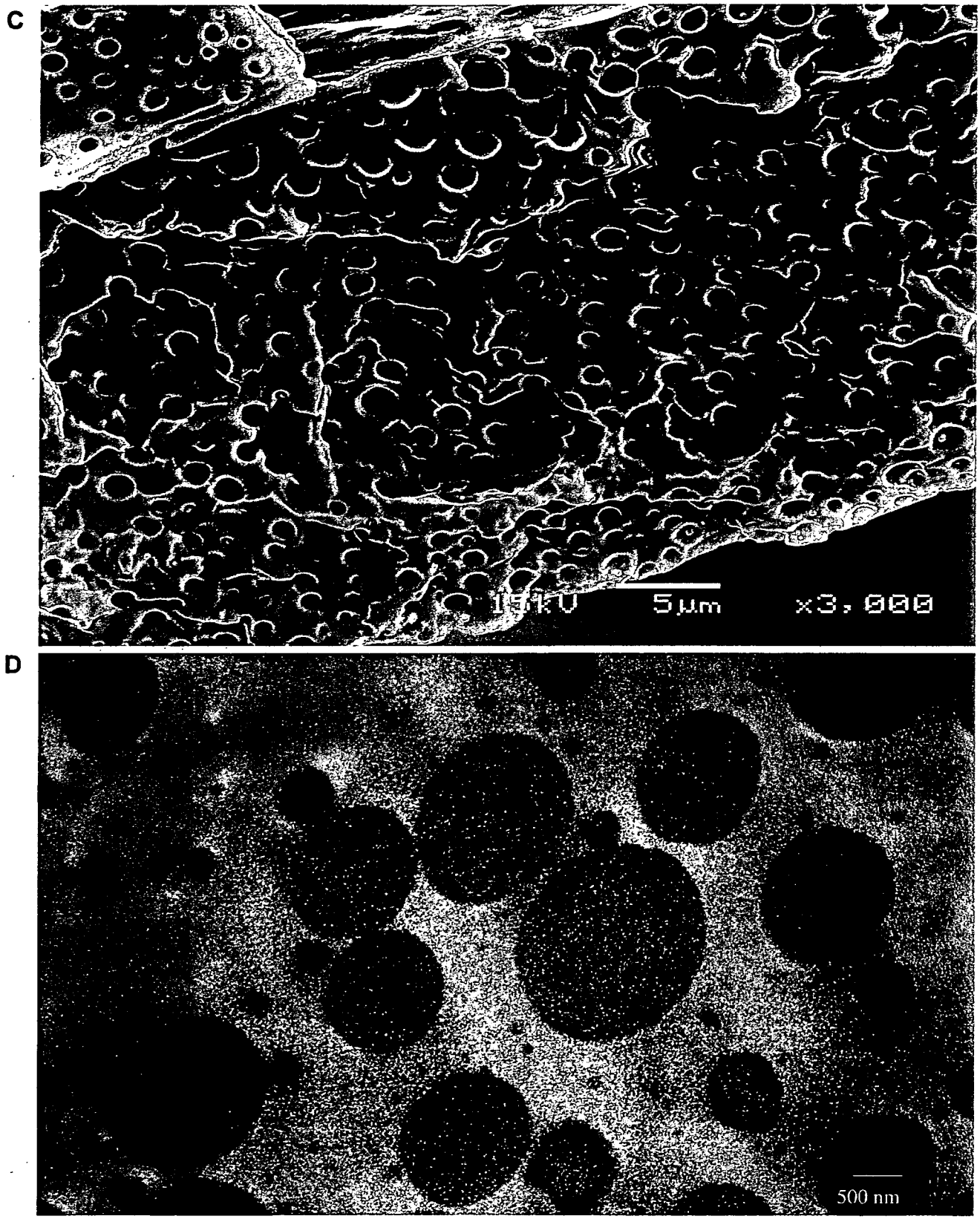

Figure 4. *continued*

on days 14 and 17 (p=0.064 and 0.019, respectively). The sizes of tumors treated with the doxorubicin sheet were comparable to those of animals treated by direct injection with a 4-times higher total dose (on day 14: injection 4.88±2.33 cm^3 *vs.* sheet 5.50±1.81 cm^3, on day 17: 14.80±6.62 cm^3 *vs.* 12.56±2.65 cm^3).

Morphological studies of the sheet. The sheet's ability to confer toxicity to the target tumor by releasing the drug was confirmed. To further investigate the material, the sheet was examined by electronmicroscopy. The sheet had a thickness of 10 μm and was flexible (Figure 4A). The surface of the sheet consisted of an amorphous structure with small cavities having a diameter of 0.5 to 3 μm. A grain, presumably of drug, was held in each cavity and some of these protruded to the surface. Some of the cavities were empty, but this may have been due to elution of the drug during preparation of the specimen (Figure 4B). An ethanol-cracked, vertical section revealed the spongy, cheese-like structure of the sheet. Most of the cavity was hollow due to the same reason as above, but the drug is visible in the cavities through a small exit (Figure 4C). This finding was confirmed by transmission electronmicroscopy (Figure 4D). The structure of the sheet may be responsible for sustained release of the drug.

Discussion

In this study, a doxorubicin-loaded poly (D, L-lactide-co-glycolide) membrane was developed and drug release from the membrane, biodegradation and efficacy on implanted glioma cells were examined.

As a scaffold for drug polymerization, PLGA was chosen. Similar to other polymers (14), PLGA has been used, not only as biodegradable polyester elastomers in tissue engineering (15), but also as a carrier of drugs, antigens, or genes either by itself or in combination with other appropriate materials. Owing to its safety, performance, cost and ease-of-use, this material was especially useful as a drug delivery tool for anticancer drugs. Micro- or nano-particles of PLGA conjugates include paclitaxel (16-20), doxorubicin (21-23), floxuridine (24), cystatins (25), camptothetin (26), 5-fluorouracil (27, 28), oxaliplatin (29), methotrexate (30) and cisplatin (31). In addition to the anticancer agents, tumor antigen (32, 33), photodynamic (34-37) or radiosensitizer (38, 39), genes (40-42) or DNA decoys (43), anti-angiogenic agents (44, 45), usnic acid (46), interferons (47), immunotoxin (48), all-trans retinoic acid (49), hormones (42, 50) and other compounds have been conjugated to PLGA for the treatment of malignant diseases.

Nano- or micro-particles of PLGA have drug delivery advantages, such as achievement of a higher concentration in the target tissue, sustained release and a longer circulation time in plasma as well as lower toxicity. However, from the stand-point of brain tumor therapy, especially considering the prevention of recurrence, there is an advantage of local therapy with an implantable drug-conjugated device, even though diffusion of nanoparticles is relatively limited to the vicinity of the implantation site (27). Accordingly, a wafer with BCNU was successfully developed (7, 8, 51). In other solid tumors, local treatment with PLGA polymers with paclitaxel and vinca alkaloid were developed and tested in clinical pilot trials (52, 53).

We chose doxorubicin for co-polymerization to PLGA. This drug has a long history and has been used widely for the treatment of malignancies, including leukemias, lymphomas and many solid tumors, including brain tumors. Accordingly, its pharmacokinetics are well known. From the aspect of safety, the drug can be administrated intrathecally with few serious adverse effects (54, 55). This might compromise safety if leakage of the drug occurs into the cerebrospinal fluid. Moreover, resistance to alkylating agent due mainly to overexpression of MGMT generally does not demonstrate cross-resistance to doxorubicin, which blocks DNA and RNA synthesis by inhibiting topoisomerase II. The sheet might be especially useful for patients with recurrent drug-resistant gliomas initially treated by alkylating agents.

Local therapies are key options for the treatment of brain tumors. BCNU-loaded wafers and other implantable nano- and micro-particles are the materials of first choice. It is preferable to increase the number of effective devices or drugs for local treatment. Since our PLGA-based sheet is implantable, easy to prepare, wholly degradable and displays a sustained-release property, it may play a role in the treatment for malignant brain tumors as a local therapy device.

Acknowledgements

The work was partly supported by a Grant-in-Aid for the Third Term Comprehensive Control Research for Cancer. We thank Hideki Saito, Emi Kikuchi and Yuko Abe in the Jikei University School of Medicine, Japan, for skillful technical assistances.

References

1 Ohgaki H and Kleihues P: Population-based studies on incidence, survival rates, and genetic alterations in astrocytic and oligodendroglial gliomas. J Neuropathol Exp Neurol *64*: 479-489, 2005.

2 Barrie M, Couprie C, Dufour H, Figarella-Branger D, Muracciole X, Hoang-Xuan K, Braguer D, Martin PM, Peragut JC, Grisoli F and Chinot O: Temozolomide in combination with BCNU before and after radiotherapy in patients with inoperable newly diagnosed glioblastoma multiforme. Ann Oncol *16*: 1177-1184, 2005.

3 Cohen MH, Johnson JR and Pazdur R: Food and Drug Administration Drug approval summary: temozolomide plus radiation therapy for the treatment of newly diagnosed glioblastoma multiforme. Clin Cancer Res *11*: 6767-6771, 2005.

4 Yoshii Y, Maki Y, Tsuboi K, Tomono Y, Nakagawa K and Hoshino T: Estimation of growth fraction with bromodeoxyuridine in human central nervous system tumors. J Neurosurg *65*: 659-663, 1986.

5 Hamstra DA, Moffat BA, Hall DE, Young JM, Desmond TJ, Carter J, Pietronigro D, Frey KA, Rehemtulla A and Ross BD: Intratumoral injection of BCNU in ethanol (DTI-015) results in enhanced delivery to tumor – a pharmacokinetic study. J Neurooncol *73*: 225-238, 2005.

6 Yimam MA, Bui T and Ho RJ: Effects of lipid association on lomustine (CCNU) administered intracerebrally to syngeneic 36B-10 rat brain tumors. Cancer Lett, 2006.

7 Seong H, An TK, Khang G, Choi SU, Lee CO and Lee HB: BCNU-loaded poly(D, L-lactide-co-glycolide) wafer and antitumor activity against XF-498 human CNS tumor cells *in vitro*. Int J Pharm *251*: 1-12, 2003.

8 Lee JS, An TK, Chae GS, Jeong JK, Cho SH, Lee HB and Khang G: Evaluation of *in vitro* and *in vivo* antitumor activity of BCNU-loaded PLGA wafer against 9L gliosarcoma. Eur J Pharm Biopharm *59*: 169-175, 2005.

9 Westphal M, Hilt DC, Bortey E, Delavault P, Olivares R, Warnke PC, Whittle IR, Jaaskelainen J and Ram Z: A phase 3 trial of local chemotherapy with biodegradable carmustine (BCNU) wafers (Gliadel wafers) in patients with primary malignant glioma. Neuro-oncol *5*: 79-88, 2003.

10 Bobola MS, Silber JR, Ellenbogen RG, Geyer JR, Blank A and Goff RD: O6-methylguanine-DNA methyltransferase, O_6-benzylguanine, and resistance to clinical alkylators in pediatric primary brain tumor cell lines. Clin Cancer Res *11*: 2747-2755, 2005.

11 Hermisson M, Klumpp A, Wick W, Wischhusen J, Nagel G, Roos W, Kaina B and Weller M: O_6-methylguanine DNA methyltransferase and p53 status predict temozolomide sensitivity in human malignant glioma cells. J Neurochem *96*: 766-776, 2006.

12 Manome Y, Watanabe M, Futaki K, Ishiguro H, Iwagami S, Noda K, Dobashi H, Ochiai Y, Ohara Y, Sanuki K, Kunieda T and Ohno T: Development of a syngenic brain-tumor model resistant to chloroethyl-nitrosourea using a methylguanine DNA methyltransferase cDNA. Anticancer Res *19*: 5313-5318, 1999.

13 Manome Y, Yoshinaga H, Watanabe M and Ohno T: Adenoviral transfer of antisenses or ribozyme to O_6-methylguanine-DNA methyltransferase mRNA in brain-tumor model resistant to chloroethyl-nitrosourea. Anticancer Res *22*: 2029-2036, 2002.

14 Lesniak MS, Upadhyay U, Goodwin R, Tyler B and Brem H: Local delivery of doxorubicin for the treatment of malignant brain tumors in rats. Anticancer Res *25*: 3825-3831, 2005.

15 Webb AR, Yang J and Ameer GA: Biodegradable polyester elastomers in tissue engineering. Expert Opin Biol Ther *4*: 801-812, 2004.

16 Fonseca C, Simoes S and Gaspar R: Paclitaxel-loaded PLGA nanoparticles: preparation, physicochemical characterization and *in vitro* anti-tumoral activity. J Control Release *83*: 273-286, 2002.

17 Kang BK, Chon SK, Kim SH, Jeong S, Kim MS, Cho SH, Lee HB and Khang G: Controlled release of paclitaxel from microemulsion containing PLGA and evaluation of anti-tumor activity *in vitro* and *in vivo*. Int J Pharm *286*: 147-156, 2004.

18 Mo Y and Lim LY: Paclitaxel-loaded PLGA nanoparticles: potentiation of anticancer activity by surface conjugation with wheat germ agglutinin. J Control Release *108*: 244-262, 2005.

19 Mo Y and Lim LY: Preparation and *in vitro* anticancer activity of wheat germ agglutinin (WGA)-conjugated PLGA nanoparticles loaded with paclitaxel and isopropyl myristate. J Control Release. *107*: 30-42, 2005.

20 Sahoo SK and Labhasetwar V: Enhanced antiproliferative activity of transferrin-conjugated paclitaxel-loaded nanoparticles is mediated *via* sustained intracellular drug retention. Mol Pharm *2*: 373-383, 2005.

21 Lin R, Shi Ng L and Wang CH: *In vitro* study of anticancer drug doxorubicin in PLGA-based microparticles. Biomaterials *26*: 4476-4485, 2005.

22 Yoo HS and Park TG: Biodegradable polymeric micelles composed of doxorubicin conjugated PLGA-PEG block copolymer. J Control Release *70*: 63-70, 2001.

23 Mallery SR, Pei P, Kang J, Ness GM, Ortiz R, Touhalisky JE and Schwendeman SP: Controlled-release of doxorubicin from poly(lactide-co-glycolide) microspheres significantly enhances cytotoxicity against cultured AIDS-related Kaposi's sarcoma cells. Anticancer Res *20*: 2817-2825, 2000.

24 Inoue K, Onishi H, Kato Y, Michiura T, Nakai K, Sato M, Yamamichi K, Machida Y and Nakane Y: Comparison of intraperitoneal continuous infusion of floxuridine and bolus administration in a peritoneal gastric cancer xenograft model. Cancer Chemother Pharmacol *53*: 415-422, 2004.

25 Cegnar M, Premzl A, Zavasnik-Bergant V, Kristl J and Kos J: Poly(lactide-co-glycolide) nanoparticles as a carrier system for delivering cysteine protease inhibitor cystatin into tumor cells. Exp Cell Res *301*: 223-231, 2004.

26 Tong W, Wang L and D'Souza MJ: Evaluation of PLGA microspheres as delivery system for antitumor agent-camptothecin. Drug Dev Ind Pharm *29*: 745-756, 2003.

27 Roullin VG, Deverre JR, Lemaire L, Hindre F, Venier-Julienne MC, Vienet R and Benoit JP: Anti-cancer drug diffusion within living rat brain tissue: an experimental study using [^{3}H](6)-5-fluorouracil-loaded PLGA microspheres. Eur J Pharm Biopharm *53*: 293-299, 2002.

28 Hagiwara A, Sakakura C, Shirasu M, Yamasaki J, Togawa T, Takahashi T, Muranishi S, Hyon S and Ikada Y: Therapeutic effects of 5-fluorouracil microspheres on peritoneal carcinomatosis induced by Colon 26 or B-16 melanoma in mice. Anticancer Drugs *9*: 287-289, 1998.

29 Lagarce F, Cruaud O, Deuschel C, Bayssas M, Griffon-Etienne G and Benoit J: Oxaliplatin loaded PLAGA microspheres: design of specific release profiles. Int J Pharm *242*: 243-246, 2002.

30 Singh UV and Udupa N: *In vitro* characterization of methotrexate loaded poly(lactic-co-glycolic) acid microspheres and antitumor efficacy in Sarcoma-180 mice bearing tumor. Pharm Acta Helv *72*: 165-173, 1997.

31 Kumagai S, Sugiyama T, Nishida T, Ushijima K and Yakushiji M: Improvement of intraperitoneal chemotherapy for rat ovarian cancer using cisplatin-containing microspheres. Jpn J Cancer Res *87*: 412-417, 1996.

32 Waeckerle-Men Y and Groettrup M: PLGA microspheres for improved antigen delivery to dendritic cells as cellular vaccines. Adv Drug Deliv Rev *57*: 475-482, 2005.

33 Waeckerle-Men Y, Scandella E, Uetz-Von Allmen E, Ludewig B, Gillessen S, Merkle HP, Gander B and Groettrup M: Phenotype and functional analysis of human monocyte-derived dendritic cells loaded with biodegradable poly(lactide-co-glycolide) microspheres for immunotherapy. J Immunol Methods *287*: 109-124, 2004.

34 McCarthy JR, Perez JM, Bruckner C and Weissleder R: Polymeric nanoparticle preparation that eradicates tumors. Nano Lett *5*: 2552-2556, 2005.

35 Vargas A, Pegaz B, Debefve E, Konan-Kouakou Y, Lange N, Ballini JP, van den Bergh H, Gurny R and Delie F: Improved photodynamic activity of porphyrin loaded into nanoparticles: an *in vivo* evaluation using chick embryos. Int J Pharm *286*: 131-145, 2004.

36 Konan YN, Berton M, Gurny R and Allemann E: Enhanced photodynamic activity of meso-tetra(4-hydroxyphenyl)porphyrin by incorporation into sub-200 nm nanoparticles. Eur J Pharm Sci *18*: 241-249, 2003.

37 Konan YN, Chevallier J, Gurny R and Allemann E: Encapsulation of p-THPP into nanoparticles: cellular uptake, subcellular localization and effect of serum on photodynamic activity. Photochem Photobiol *77*: 638-644, 2003.

38 Geze A, Venier-Julienne MC, Saulnier P, Varlet P, Daumas-Duport C, Devauchelle P and Benoit JP: Modulated release of IdUrd from poly (D,L-lactide-co-glycolide) microspheres by addition of poly (D,L-lactide) oligomers. J Control Release *58*: 311-322, 1999.

39 Reza MS and Whateley TL: Iodo-2'-deoxyuridine (IUdR) and 125IUdR loaded biodegradable microspheres for controlled delivery to the brain. J Microencapsul *15*: 789-801, 1998.

40 Prabha S and Labhasetwar V: Critical determinants in PLGA/PLA nanoparticle-mediated gene expression. Pharm Res *21*: 354-364, 2004.

41 Jilek S, Ulrich M, Merkle HP and Walter E: Composition and surface charge of DNA-loaded microparticles determine maturation and cytokine secretion in human dendritic cells. Pharm Res *21*: 1240-1247, 2004.

42 Panyam J, Zhou WZ, Prabha S, Sahoo SK and Labhasetwar V: Rapid endo-lysosomal escape of poly(DL-lactide-co-glycolide) nanoparticles: implications for drug and gene delivery. Faseb J *16*: 1217-1226, 2002.

43 Gill JS, Zhu X, Moore MJ, Lu L, Yaszemski MJ and Windebank AJ: Effects of NFkappaB decoy oligonucleotides released from biodegradable polymer microparticles on a glioblastoma cell line. Biomaterials *23*: 2773-2781, 2002.

44 Benny O, Duvshani-Eshet M, Cargioli T, Bello L, Bikfalvi A, Carroll RS and Machluf M: Continuous delivery of endogenous inhibitors from poly(lactic-co-glycolic acid) polymeric microspheres inhibits glioma tumor growth. Clin Cancer Res *11*: 768-776, 2005.

45 Bandi N, Ayalasomayajula SP, Dhanda DS, Iwakawa J, Cheng PW and Kompella UB: Intratracheal budesonide-poly(lactide-co-glycolide) microparticles reduce oxidative stress, VEGF expression, and vascular leakage in a benzo(a)pyrene-fed mouse model. J Pharm Pharmacol *57*: 851-860, 2005.

46 Ribeiro-Costa RM, Alves AJ, Santos NP, Nascimento SC, Goncalves EC, Silva NH, Honda NK and Santos-Magalhaes NS: *In vitro* and *in vivo* properties of usnic acid encapsulated into PLGA-microspheres. J Microencapsul *21*: 371-384, 2004.

47 Sanchez A, Tobio M, Gonzalez L, Fabra A and Alonso MJ: Biodegradable micro- and nanoparticles as long-term delivery vehicles for interferon-alpha. Eur J Pharm Sci *18*: 221-229, 2003.

48 Ferdous AJ, Stembridge NY and Singh M: Role of monensin PLGA polymer nanoparticles and liposomes as potentiator of ricin A immunotoxins *in vitro*. J Control Release *50*: 71-78, 1998.

49 Jeong YI, Song JG, Kang SS, Ryu HH, Lee YH, Choi C, Shin BA, Kim KK, Ahn KY and Jung S: Preparation of poly(DL-lactide-co-glycolide) microspheres encapsulating all-trans retinoic acid. Int J Pharm *259*: 79-91, 2003.

50 Labrie F, Li S, Belanger A, Cote J, Merand Y and Lepage M: Controlled release low dose medroxyprogesterone acetate (MPA) inhibits the development of mammary tumors induced by dimethyl-benz(a) anthracene in the rat. Breast Cancer Res Treat *26*: 253-265, 1993.

51 Chae GS, Lee JS, Kim SH, Seo KS, Kim MS, Lee HB and Khang G: Enhancement of the stability of BCNU using self-emulsifying drug delivery systems (SEDDS) and *in vitro* antitumor activity of self-emulsified BCNU-loaded PLGA wafer. Int J Pharm 301: 6-14, 2005.

52 Rohr UD, Oberhoff C, Markmann S, Gerber B, Scheulen M and Schindler AE: The safety of synthetic paclitaxel by intralesional delivery with OncoGeltrade mark into skin breast cancer metastases: method and results of a clinical pilot trial. Arch Gynecol Obstet 1-7, 2005.

53 Fournier C, Hecquet B, Bouffard P, Vert M, Caty A, Vilain MO, Vanseymortier L, Merle S, Krikorian A, Lefebvre JL *et al*: Experimental studies and preliminary clinical trial of vinorelbine-loaded polymeric bioresorbable implants for the local treatment of solid tumors. Cancer Res *51*: 5384-5391, 1991.

54 Jordan B, Pasquier Y and Schnider A: Neurological improvement and rehabilitation potential following toxic myelopathy due to intrathecal injection of doxorubicin. Spinal Cord *42*: 371-373, 2004.

55 Arico M, Nespoli L, Porta F, Caselli D, Raiteri E and Burgio GR: Severe acute encephalopathy following inadvertent intrathecal doxorubicin administration. Med Pediatr Oncol *18*: 261-263, 1990.

Received May 5, 2006
Accepted May 29, 2006

MRIの優位性はここにある

外科手術に効果大きいMR設置のMRX手術室開設と応用開始

国立がんセンター
小林寿光　中馬広一　木下貴之　宮北康二
山崎直也　下山直人　土屋了介　垣添忠生


小林氏

●Summary
A new operating room, the MRX Surgical Room, which encompasses an MRI, CT and flatpanel fluoroscopy systems, in anticipation of increasing effectiveness with regard to the results of standard surgical procedures by using imaging systems intraoperatively, has begun functioning in clinical studies.

要旨：画像装置を手術中に使用することで、標準的な外科成果に上乗せ効果を期待した、MRIやCT、フラットパネルX線透視装置を導入した新たな手術室、MRX手術室が開設され、臨床試験として応用が開始された。

MRI装置の手術室導入で目指す手術の標準化と低侵襲化

外科治療は悪性腫瘍の治癒が期待できる標準的な治療法であるが、高度な手術技術の標準化と標準的な手術の低侵襲化は重要な課題である。

一般に熟練した外科医でも難しいのは、体内深部の狭小部、また見えづらい領域であり、経験に基づく高い技術が必要である。単なる勘に頼って無理をすれば、効果と安全性が犠牲になる可能性があった。

MRX手術室開発の目的は上乗せ効果

画像装置は病変の発見から診断、手術適応の決定に使用されており、手術中に使用できれば何らかの上乗せ効果が期待される。手術を中心に考えれば画像診断室で手術ができる設備を整えるのではなく、これまでの手術室環境を保ったまま画像装置を導入する必要がある。

確かに画像装置を使用した新たな放射線科的な医療技術開発や[1,2]、脳神経外科などの医療技術を高度化することには非常に大きな意義がある[3,4]。しかし医療施設全体として導入経費と成果のバランスを取るためには、幅広い外科領域に対する汎用手術室として構築する必要がある。

以上の必要性から、新たな画像補助手術室は、既存の手術室フロアの一角に導入されることとなった。

手術室に導入する画像機器装置はMRIにCT、FPD

導入する画像装置は手術適応を決定するために使用されるものの中で、手術室の建設時に設置が必要なMRIとCT、X線透視装置とした。基準とするものを最も導入が難しいMRIとして、できるだけ幅広い周囲からアプローチできるオープン型とした。当初は軽量の0・2Tモデルを考えていたが、広いガントリー開口部上下幅（43㎝）を得るために0・3Tモデルとした。

CTはMRIと必要に応じて同期して運用することにも配慮したが、撮影時に術野や外科医の移動のみならず、麻酔などの配管や点滴ライン、心電図などのケーブルのつながった患者の移動を避けるために、自走式のマルチスライス（4列）ヘリカルCTを選定した。

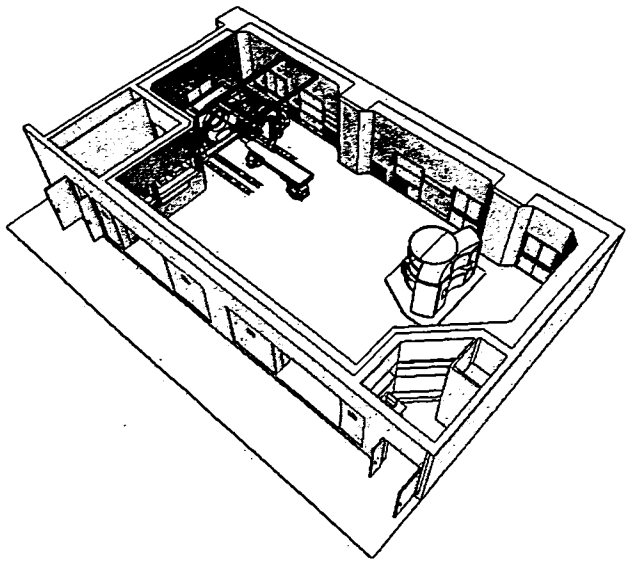

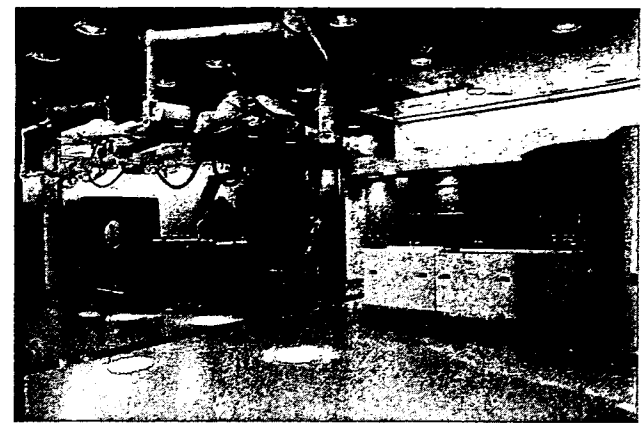

図1　右はMRX手術室、左は同手術室の3次元イメージ図

X線透視装置はこれまでも術中に使用されてきたが、コンパクトでコーンビームCTが可能なフラットパネルX線透視装置（FPD）とした。この装置はCT装置と検査・手術台を共有して、いわゆるIVR-CT/Angio装置の形態をとることとした。

共用手術スペースの確保の鍵は開閉式電磁波シールドカーテンの開発

MRIへの電磁波干渉を防止するには通常X線系装置を別室に配置するが、限られたスペース内で十分な手術スペースの確保が難しくなり、また全身麻酔下の患者移動にリスクが発生する。画像装置をすべて同室に設置した場合、X線系装置の電源を落とせば電磁波干渉を防止できるが、CTの立ち上げ時にキャリブレーションによる放射線被曝の問題等が発生する。そこでこれらX線系装置を囲み込む、開閉式電磁波シールドカーテンを開発することとした。

これを前提にしてMRI装置とX線系装置を手術室内の左右、入り口の反対側に寄せて設置することで、中央に広い共用手術スペースを確保した。将来この手術室の中央を開閉式間仕切りで分けて2室運用する可能性も考え、それぞれの操作室は左右に分けて設置することとした。

大問題なのは診療業務中に導入工事を行うこと

以上の計画からMRIの重量は約16トンで、手術室の総重量は約40トンに至ることが確認された。問題は当センター中央病院の床の耐荷重であり、床補強が建物の設計上可能であるかは大きな懸案であった。これは柱の間に設置された主梁を中心に、H鋼による補強を行うことで対処可能と計算され、結果として床面は25㎝挙上された。また40トンの重量が19階建ての建物全体に及ぼす影響も、特に問題がないことが計算上確認された。

実際の導入工事を行う点で大きな問題は、病院が診療業務中であることである。各種工事区画や必要な人材、資材の出入りは患者動線に支障を与え、工事に伴う振動や騒音は隣接する手術室や階下のICUへの影響が懸念された。特に手術室は最も活性度の高い病院機能を持ち、各種医療ガスや信号配線、電源等に関連して、病院全体に影響し得ることが問題であった。

そこで手術フロアを含め工事区画を仕切り、器材の搬入を含めたエレベーター等の動線を患者診療用と離して設置した。また騒音、振動に関しては代表的な作業を極短時間シミュレーションしてその程度を評価したが、機器や工法の工夫で絶対量を抑えるとともに、土日の施工や部屋の適切な運用で対処が可能となった。また安全に最大限配慮した工事計画を作成することはもとより、万が一の事態を想定した高度なリスクマネージメントプランを作成し、単なる研究班のみならず病院組織との連携をとることで導入工事を進めた。

重量のあるMRIの搬入は通常のエレベーターが使用できないため、病院に併置して9

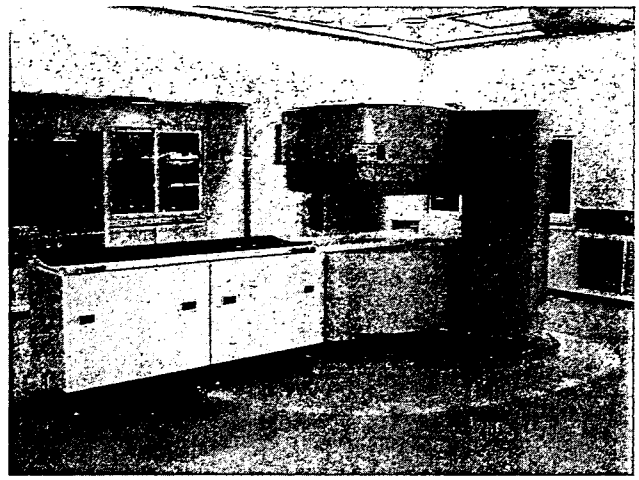

図2　床面から挙上して設置したMRI

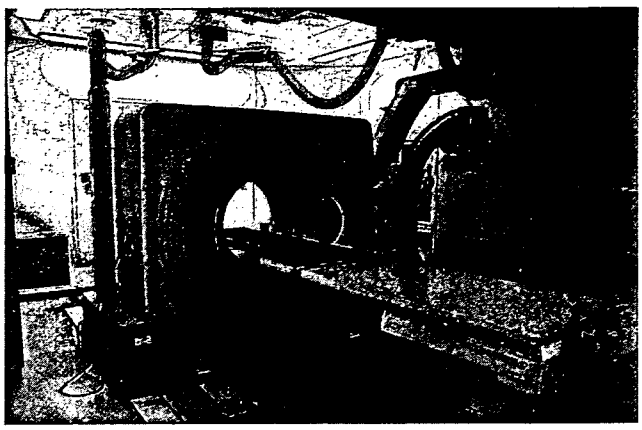

図3a　自走して手術台上の患者を撮影するCT

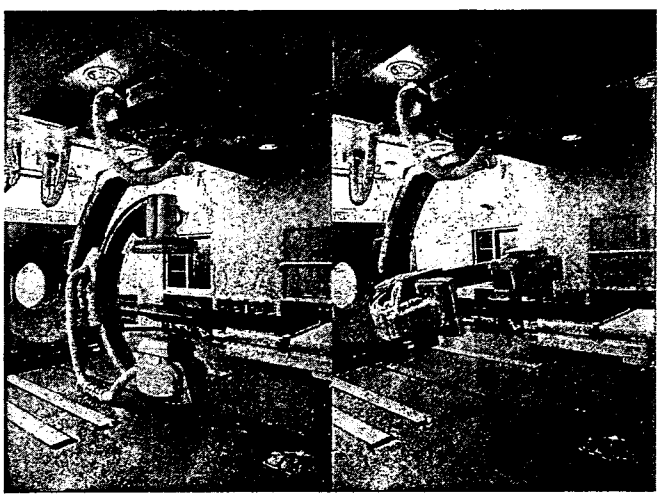

図3b　FPDによる、コーンビームCTを含めた撮影が可能

階までのエレベーターを仮設することを当初考えたが、工期や影響、コストを考えて360トン自走クレーンを使用することとした。幸運にもクレーンの進入、組み立てスペースが確保でき、地面の耐荷重補強を行い周囲側壁などへの影響も少ないと計算された。

この導入プランに従いゴールデンウィークの休診中に、何ら問題なしにMRIは搬入された。また、外壁を外した開口部は、他の建築資材の搬入にも使用された後に閉鎖された。

開設されたMRX手術室

新たな画像補助手術室は05年8月1日にMRX手術室として開設された（図1）。空調用ダクトや各種配管、配線、構造材を適切に配置することで、柱間のスペースも室内空間として利用して、十分な共用手術スペースを確保していることが特長である。床は通常の手術室と同様に、安全に配慮して段差は基本的にない。無影灯は共用手術スペースに、2室運用に配慮して2器を設置している。

X線系装置側の床にある金属ベルトは開閉式電磁波シールドカーテンの接点であり、ここに降りたカーテンは金属ベルト下の電磁石により吸引されて、電気的に完全に隙間なく閉鎖される。また室内中央を一周する金属ベルトは、将来の2室運用時に昇降式電磁波・X線両用シールドを装備するためのスペースと補強である。

MRI装置は手術時の高さを合わせるために、床面から挙上して設置した（図2）。通常の床の淡緑色と分け、5ガウスラインは乳白色の床材を使用した。また天井に赤色のLEDを設置して5ガウスライン上を照らして、不用意に5ガウスライン内に侵入したときに赤く照らされることで警告を発するようにしている。MRI用手術台は、MRIのガントリー上の平面を周囲に拡大する概念で、新規に組み合わせボックス式として開発している。

CT装置は自走して手術台上の患者を撮影するが、走行用レールは床に埋めるとともに、血液などの侵入を防ぐため表面を被覆している（図3a）。CTを撮影する場合は、FPDを壁面近くに退避させる。CTを退避させればFPD装置が手術台を囲み込み、コーンビームCTを含めた撮影が可能である

（図3b）。

X線系装置の手術台は一見診断装置の検査台のように見えるが、手術操作を補助すると共に血液などによる汚染を防止するため、検査台の天板を非常に薄い手術台で覆っている。現時点で手術台と画像装置の同期の問題などがあり、このような形態となっているが、将来は専用の手術台を開発する予定である。なお開設時には共用手術台を用意していなかったが、X線系装置とMRI装置に適合すると共に、統合可能な手術台の開発を開始している。

MRX手術室の設備はすべて使用中でもMRI画像が撮影できる、MRIとの完全適合性の獲得を原則としている。今回新規に開発したものはビデオカメラ付無影灯、MRI用手術台、X線系装置用手術台、5ガウスライン明示用LED赤色灯、ビデオカメラ付手術用顕微鏡、手術顕微鏡用段差解消用昇降台、モニター用電磁波シールドボックス、HDTVカメラ用電磁波シールドボックス、段差解消用患者移送台、開閉式電磁波シールドカーテン等である。

MRX手術室での医療行為はすべて臨床試験

医療技術と画像機器装置の開発のために、MRX手術室での医療行為はすべて臨床試験として倫理審査委員会の承認を得るものとした。脳神経外科と整形外科、乳腺外科を最初のグループとして、包括的臨床試験計画が作成された。第1評価項目は、これらの画像機器を使用した場合の標準的な外科手技への上乗せ効果の有無と、有害事象発生の有無とした。第2評価項目は、有益な術中画像情報発生の有無、使用開始後の必要に応じた使用中止の可否とした。

最初の一例は乳腺外科から開始されたが、さらに適応の拡大を図り麻酔科や看護師、診療放射線技師の協力を得て、支援体制の強化を行っている。特にMRI環境下での手術の安全指針は、今後の標準化を念頭に置いて作成している。また種々の領域に臨床応用を拡大するために、皮膚科での臨床試験を作成して倫理審査委員会に提出した。

一般的に画像補助手術と皮膚科疾患は最も距離があると考えられるが、悪性黒色腫の進展形式の特徴とMRIの特徴を組み合わせることで、有意義かつ興味ある臨床試験計画として将来その成果を発表していく予定である。

高度な姿を目標に進歩するMRX手術室

開設されたばかりでまだ開発の余地を多く残しているMRX手術室であるが、将来の高度な手術室の姿を目標に常に進歩していく手術室でもある。今後、段階的に開発されていく手術台や、階下の支援室と電子回線で結んだ新たな画像解析補助概念とシステムの開発は、その具体例である。

今後、画像補助下外科技術の開発はもとより、画像適合型ロボット手術装置の開発も促進していくと期待される。また標準的な外科成果の上乗せ効果に関しては、例えば術中MRI撮影加算などの形で保険診療化されることが重要と考えられる。

なおこのMRX手術室は手術場ユニットとして、厚生労働科学研究費補助金、身体機能解析・補助・代替機器開発研究事業、「新たな手術用ロボット装置の開発に関する研究」（主任研究者：国立がんセンター総長　垣添忠生）、及び国立がんセンターと日立メディコとの共同研究契約に基づいて導入された。

文献

1 Carino JA, Jolesz FA. MRI-guided interventions. Acad Radiol 12: 1063-1064, 2005.
2 Truwit CL, Liu H. Prospective stereotaxy: A novel method of trajectory alignment using real-time image guidance. J Magn Reson Imaging 13: 452-457, 2001.
3 Iseki H, Muragaki Y, Nakamura R, et al. Intelligent operating theater using intraoperative open-MRI. Magn Reson Med Sci 4 (3) 129-136, 2005
4 Morikawa S, Inubushi T, Kurumi Y, et al. MR-guided microwave thermocoagulation therapy of liver tumors: Initial clinical experiences using a 0.5T open MR system. J Magn Reson Imaging 16: 576-583, 2002.

※　※

小林剣光（こばやし・としあき）●59年静岡県生まれ。85年東京医科大卒。同大外科を経て、95年国立がんセンター中央病院内視鏡部呼吸器科、02年同気管支内視鏡室医長。04年から同センターがん予防・検診研究センター検診技術開発部診断支援技術開発室長。

Sentinel node navigation segmentectomy for clinical stage IA non–small cell lung cancer

Hiroaki Nomori, MD, PhD,[a] Koei Ikeda, MD, PhD,[a] Takeshi Mori, MD,[a] Hironori Kobayashi, MD,[a] Kazunori Iwatani, MD,[a] Koichi Kawanaka, MD, PhD,[b] Shinya Shiraishi, MD, PhD,[b] and Toshiaki Kobayashi, MD, PhD[c]

From right to left: Drs Nomori, Mori, and Ikeda. The Bronze statue is Dr Shibasaburo Kitasato

Objective: Intraoperative frozen section examination of sentinel lymph nodes was conducted to determine the final indication for segmentectomy for clinical T1 N0 M0 non–small cell lung cancer.

Methods: Between April 2005 and July 2006, 52 patients with clinical T1 N0 M0 non–small cell lung cancer were prospectively treated by segmentectomy with sentinel node identification. The day before surgery, technetium-99m tin colloid was injected into the peritumoral region. After segmentectomy and lymph node dissection, sentinel nodes identified by measuring radioactive tracer uptake were examined for intraoperative frozen sections, which were serially cut 2 to 3 mm in thickness. When sentinel node metastasis was observed, segmentectomy was converted to lobectomy.

Results: Sentinel nodes were identified in 43 (83%) patients. The average number of sentinel nodes was 1.6 ± 0.9 (range: 1–5) per patient. Of 3 patients with metastatic sentinel lymph nodes, 2 underwent lobectomy and 1 larger segmentectomy. None of the other 40 patients had metastatic sentinel lymph nodes and therefore they were treated with segmentectomy. Pathologic staging with permanent sections was N0 in all of the 40 patients. On the other hand, in 9 patients whose sentinel nodes could not be identified, intraoperative frozen sections were required for 5.4 ± 2.3 lymph nodes, which was significantly more than 1.6 ± 0.9 in the 43 patients with sentinel node identification ($P < .001$).

Conclusion: Sentinel node identification is useful to determine the final indication of segmentectomy for clinical T1 N0 M0 non–small cell lung cancer by targeting the lymph nodes needed for intraoperative frozen section diagnosis.

From the Departments of Thoracic Surgery[a] and Radiology,[b] Graduate School of Medical Sciences, Kumamoto University, Honjo, Kumamoto, Japan; and the Department of Assistive Diagnostic Technology,[c] National Cancer Center Hospital, Tokyo, Japan.

This work was supported, in part, by Grant-in-Aid from the Ministry of Health, Labor, and Welfare, Japan.

Received for publication Aug 20, 2006; revisions received Oct 7, 2006; accepted for publication Oct 23, 2006.

Address for reprints: Hiroaki Nomori, MD, PhD, Department of Thoracic Surgery, Graduate School of Medical Sciences, Kumamoto University, 1-1-1 Honjo, Kumamoto 860-8556, Japan (E-mail: hnomori@qk9.so-net.ne.jp).

J Thorac Cardiovasc Surg 2007;133:780-5

0022-5223/$32.00

doi:10.1016/j.jtcvs.2006.10.027

GTS

In 1995, the Lung Cancer Study Group[1] conducted a prospective randomized controlled trial of limited resection versus lobectomy for clinical T1 N0 M0 non–small cell lung cancer (NSCLC) and concluded that the former was inferior to the latter regarding local recurrence and survival. However, the limited resection group in the study included both segmentectomy and wedge resection, and the curability for T1 N0 M0 NSCLC differed between the two procedures. On the other hand, there have been several reports describing that survivals were similar between patients treated with segmentectomy and those with lobectomy.[2-7]

The most important issue regarding segmentectomy versus lobectomy is whether postoperative local recurrence is increased. Whereas Warren and Faber[8] reported local recurrence in 15 (22.7%) of 66 patients after segmentectomy versus 5 (4.9%) of 103 patients after lobectomy, other authors reported that local recurrence after segmentectomy with complete dissection of hilar and mediastinal lymph nodes was equal to that after lobectomy.[3-6] However, for determining the final indication for segmentectomy, intraoperative frozen sections must be examined for all of the hilar

Abbreviations and Acronyms

CT = computed tomography
FDG-PET = fluorodeoxyglucose–positron emission tomography
NSCLC = non–small cell lung cancer
SN = sentinel node
SPECT = single photon emission computed tomography

and lobe-specific mediastinal lymph nodes to confirm the intraoperative N staging to be N0.[3-6]

A sentinel node (SN) is defined as the first lymph node within the lymphatic basin reached by lymph draining from the primary lesion. Recently, SNs have been identified by a radioactive tracer with or without dye during surgery for melanoma, breast cancer, gastrointestinal cancer, and lung cancer to reduce lymph node dissection.[9-14] We[13,14] previously reported that SN identification with technetium-99m tin colloid could establish the first site of nodal metastasis in NSCLC.

In the present study, we used SN identification to target the lymph nodes submitted for intraoperative frozen section diagnosis, which might determine the indication of segmentectomy. In addition, unlike Tsubota,[3] Okada,[4] Yoshikawa,[5] and their associates, who proposed that the indication for segmentectomy was T1 N0 M0 NSCLC less than 2 cm in size, we proposed that it was T1 N0 M0 NSCLC without size limitation. Because SN identification served as the final indication of segmentectomy, we named the procedure "sentinel node navigation segmentectomy."

Patients and Methods

Eligibility

The study protocol for SN navigation segmentectomy was approved by the Ethics Committee of Kumamoto University Hospital in March 2005. Informed consent was obtained from all patients after discussing the risks and benefits of the proposed surgery with their surgeons.

Patients

Between April 2005 and July 2006, 103 patients with NSCLC underwent surgical treatment. Of these, 73 patients had stage c-T1 N0 M0 cancer according to the findings of both computed tomography (CT) and fluorodeoxyglucose–positron emission tomography (FDG-PET). SN navigation segmentectomy was prospectively performed when (1) c-T1 N0 M0 NSCLC was identified in the peripheral lung; (2) the tumor on CT was more than 2 cm away from the pulmonary vein running at the boundary of the affected segment; (3) intraoperative frozen sections of SN showed no metastasis; (4) the surgical margin was intraoperatively found to be more than 2 cm from the tumor; and (5) tumors located centrally within the inner one third of the lung or in the right middle lobe were excluded. The stage of disease was based on the TNM classification of the International Union Against Cancer.[15] The lymph node nomenclature used was according to the lymph node map of Naruke and associates,[16] which was approved by the Japan Lung Cancer Society (Table 1).

TABLE 1. Lymph node nomenclature

N2 node	N1 node
Superior mediastinal	Hilar
No. 1. Highest mediastinal	No. 10. Hilar
No. 2. Paratracheal	No. 11. Interlobar
No. 3. Pretracheal	No. 12. Lobar
No. 4. Tracheobronchial	
Aortic	Intrapulmonary
No. 5. Botallo	No. 13. Segmental
No. 6. Para-aortic	No. 14. Subsegmental
Inferior mediastinal	
No. 7. Subcarinal	
No. 8. Paraesophageal	
No. 9. Pulmonary ligament	

Administration of Radioactive Colloid

The day before surgery, a 23-gauge needle was introduced into the peritumoral region under single photon emission computed tomography/computed tomography (SPECT/CT) system guidance, which incorporates a gantry-free SPECT with dual-head detectors (Skylight; ADAC Laboratories, Milpitas, Calif) and an 8 multidetector CT scanner (Light-Speed Ultra; General Electrics, Milwaukee, Wis). Technetium tin colloid (6–8 mCi) suspended in a 1- to 1.5-mL volume was injected in a single shot. SPECT/CT was performed 5 minutes after the injection and the next morning just before the operation.

SN Identification

The radioactivity of the resected lymph nodes was counted with a handheld gamma probe (Navigator; Auto Suture Japan, Tokyo, Japan). The radioactivity was measured for a 10-second period. SN was defined as any node for which the count was more than 5 times the radioactivity of the resected tissue with the lowest count.

SN Navigation Segmentectomy

Under thoracotomy, SN navigation segmentectomy was performed as follows: (1) Pulmonary arteries and bronchi of the affected segments were cut at the hilum; (2) pulmonary veins along the boundary of segments were isolated from the center to periphery; (3) the affected segments along the pulmonary veins were resected with staplers; (4) the hilar and systematic mediastinal lymph nodes were dissected; (5) the radioactivity of dissected lymph nodes was counted for SN identification; (6) SNs were examined by intraoperative frozen sections, which were serially cut 2 to 3 mm in thickness; (7) if the intraoperative frozen sections of the SN showed no metastasis, the operation was completed with segmentectomy; (8) if the sections of the SN showed metastasis, lobectomy was performed; and (9) if the SN could not be identified because radioactivity of the lymph nodes was low, all of the hilar and lobe-specific mediastinal lymph nodes were submitted for

GTS

TABLE 2. Sites of segmentectomy

Segment	No. of patients	Segment	No. of patients
Right		Left	
Upper lobe		Upper lobe	
S1	3	S1 + 2	4
S2	2	S3	2
S1 + S2	2	S1 + 2 + 3	9
S3	2	S4 + 5	7
S3 + S2b	1		
S2 + S3a	1		
Lower lobe		Lower lobe	
S6	4	S6	3
S7 + 8	1	S8	1
S8	1	S8 + 9	2
S9 + S10	2	S9 + 10	1
S7–10	1	S10	1
S6 + S9 + S10	1	S8–10	1
Total	21		31

Right upper lobe: *S1*, apical; *S2*, anterior; *S3*, posterior. Right lower lobe: *S6*, apical; *S7*, medial; *S8*, anterior; *S9*, lateral; *S10*, posterior. Left upper lobe: *S1+2*, apical posterior; *S3*, apical anterior; *S4*, superior lingular; *S5*, inferior lingular. Left lower lobe: *S6*, apical; *S8*, anterior; *S9*, lateral; *S10*, posterior.

TABLE 3. Characteristics of patients with and without sentinel node identification

	Sentinel lymph node	
	Identifiable	Nonidentifiable
Mean age (y)	69 ± 7	71 ± 7
Sex		
Male	26	8
Female	17	1
Mean tumor size (cm)	1.9 ± 0.7	2.1 ± 0.7
Histologic type		
Adenocarcinoma	37	6
Squamous cell carcinoma	4	2
Adenosquamous carcinoma	2	1
No. of lymph nodes submitted for intraoperative frozen diagnosis	1.6 ± 0.9	5.4 ± 2.3*
Pathologic TNM		
T1 N0 M0	39	9
T2 N0 M0	1	0
T1 N1 M0	1	0
T2 N1 M0	1	0
T1 N2 M0	1	0
Total	43	9

*$P < .001$.

intraoperative frozen section. Lobe-specific lymph nodes were defined as follows: No. 3 and No. 4 for the right upper lobe, No. 5 for the left upper lobe, and No. 7 for the lower lobe of both sides.[17]

Primary End Points of the Study

Primary end points of the study are as follows: (1) Can SN identification diagnose pathologic N stage during segmentectomy? (2) Are the survival and local recurrence after SN navigation segmentectomy similar to those after lobectomy?

Statistical Analysis

All data were analyzed for significance by the 2-tailed Student *t* tests. All values in the text and tables are given as mean ± SD.

Results

Operative procedures for the 73 patients with c-T1 N0 M0 were lobectomy in 12 patients, segmentectomy in 52, and wedge resection in 9. The reasons for conducting lobectomy in the 12 patients were as follows: (1) tumors in the right middle lobe in 5 patients; (2) tumors located centrally in 5 patients; (3) multiple lesions in the same lobe in 1 patient; and (4) thoracoscopic lobectomy as requested by the patient. As a result, 52 patients were consecutively enrolled for SN navigation segmentectomy. Table 2 shows the sites of segmentectomy for the 52 patients. The average number of dissected lymph node stations and lymph nodes per patient was 6 ± 1.8 stations and 12.5 ± 5.9 lymph nodes, respectively. Among the 52 patients, SNs could be identified in 43 (83%). The time needed for SN identification was within 5 minutes in each patient. The characteristics of the 43 patients with SN identification and of the 9 patients without are shown in Table 3. Average tumor size on CT was 1.9 ± 0.7 cm (range: 0.8–3.0 cm) and 2.1 ± 0.7 cm (range: 1.4–3.0 cm) in the patients with and without SN identification, respectively. Seventeen (40%) of the 43 patients with SN identification and 4 (44%) of 9 patients without had tumors larger than 2 cm. Pathologic tumor stages in the 43 patients with SN identification were T1 N0 M0 in 39, T2 N0 M0 in 1, T1 N1 M0 in 1, T2 N1 M0 in 1, and T1 N2 M0 in 1, whereas the stage in all 9 patients without SN identification was p-T1 N0 M0. The tumors in 2 patients were pathologically classified as T2; one tumor was spread over the pleura and the other was more than 3 cm in size in the permanent section. The average number of lymph nodes submitted for intraoperative frozen section examination was significantly less in the 43 patients with SN identification (1.6 ± 0.9 [range: 1–5] per patient) than in the 9 patients without SN identification (5.4 ± 2.3 [range: 3–10] per patient) ($P < .001$).

Table 4 shows the SN identified in the hilar lymph node stations. The number of stations having SN increased in numeric order from No. 10 to 13 stations. In the mediastinal lymph node stations, the SN was identified in 15 of the 43 patients (35%). Eleven of the 15 patients had SNs in both the hilar and mediastinal lymph node stations, whereas the remaining 4 patients had SNs only in the mediastinum. The distribution of mediastinal SNs is shown in Table 5, which

TABLE 4. Sentinel lymph node mapping in the hilar lymph node stations

Station	Sentinel nodes	
	No. of patients	Percent
10	7/3	16.3
11	7/43	16.3
12	12/43	27.9
13	22/43	51.2

TABLE 5. Sentinel nodes at the mediastinum in each lobe

Tumor location	Station of mediastinal SN	No. of patients	Percent
RUL	3 or 4	3/10	30.0
RLL	3 or 4	2/9	22.2
	7 and 3	1/9	11.2
LUL	5	8/18	44.4
LLL	7	2/6	33.3

SN, Sentinel node; *RUL*, right upper lobe; *RLL*, right lower lobe; *LUL*, left upper lobe; *LLL*, left lower lobe.

was lobe-specific; that is, 3 of the 10 patients with primary tumor in the right upper lobe had SN in No. 3 or 4 stations; 3 of the 9 patients with primary tumor in the right lower lobe had SN in No. 7, 3, or 4 stations; 8 of the 18 patients with primary tumor in the left upper lobe had SN in No. 5 station; and 2 of the 6 patients with primary tumor in the left lower lobe had SN in No. 7 station.

In 3 (7%) of the 43 patients with SN identification, metastasis was found in the SN by intraoperative frozen section (Table 6). For 2 of the 3 patients (patients 1 and 2), operative procedures were converted to lobectomy. The operative procedure for the remaining patient (patient 3) was converted from posterior apical segmentectomy to larger segmentectomy (upper division segmentectomy, but not to upper lobectomy), because of his age (80 years old). Pathologic N stages were N1 in 2 patients and N2 in 1 patient. Although both patients 1 and 2 had metastasis only in the SN, patient 3 had metastasis in both SN (No. 5) and non-SN (Nos. 12 and 13). Tumors in all of the other 40 patients were classified as p-N0 by permanent sections.

There were no complications associated with radioisotope injection necessitating tube drainage, such as bleeding or severe pneumothorax. One patient had empyema 3 days after segmentectomy, which was cured by drainage and antibiotics on the 23rd postoperative day. There were no the other major complications associated with segmentectomy, including prolonged air leakage of more than 5 days. The postoperative follow-up was performed by chest and abdominal CT and brain magnetic resonance imaging every 3 months after the operation. No patients were lost to follow-up. The mean follow-up period after surgery in the 52 patients was 8 months (range: 1–15 months). Postoperative recurrence occurred in 1 patient, who underwent an apical segmentectomy of the right lower lobe for adenosquamous carcinoma 2.9 cm in size. The recurrence was at 5 months after segmentectomy, at the extraregional lymph node for tumor in the right lower lobe, that is, at the interlobar lymph node (No. 11) between the right upper lobe and middle lobe, and treated by completion pneumonectomy. During the segmentectomy of this patient, No. 13 and No. 4 were identified as SNs, which showed no metastasis in intraoperative frozen sections. The patient is now alive 11 months after the completion pneumonectomy without recurrence. The other 51 patients are also now alive without recurrence.

Discussion

The present study shows that the SN navigation segmentectomy using radioisotope tracers could increase the accuracy of intraoperative N staging and could serve as the final indication for segmentectomy. In the 3 patients with N1 or N2 disease, intraoperative frozen sections of SNs showed metastasis, which suggested the need for lobectomy. In 9 segmentectomy-treated patients whose SNs could not be identified, all hilar and lobe-specific lymph nodes were required for diagnosis, a significantly larger number than in the 43 patients whose SNs could be identified. SN identification therefore could determine a final indication for segmentectomy by targeting the lymph nodes needed for intraoperative frozen section diagnosis. In addition, serial sections of SNs during surgery might find micrometastasis more easily than single section in each of a larger number of lymph nodes.

Although the postoperative follow-up period is still short, 1 patient had local recurrence 5 months after segmentectomy. The recurrence site of this patient, however, was the extraregional lymph node. In addition, the histologic type of this patient was adenosquamous carcinoma, which is known to have poorer prognosis than other types of NSCLC.[18,19] We therefore consider that the patients with clinical T1 N0 M0 NSCLC of high malignant grade, such as adenosquamous carcinoma, large cell neuroendocrine carcinoma, adenocarcinoma with high FDG uptake on PET, and NSCLC with high carcinoembryonic antigen serum level, would be preferably treated by lobectomy rather than segmentectomy, even if the intraoperative lymph node staging is N0.

Skip metastasis to the mediastinal lymph nodes has been reported to occur in 20% to 40% of patients with NSCLC,[17,20] which could be because some lymphatic flow from the lung goes directly to the mediastinum through the pleura and not to the hilar lymph node stations.[21] The present study showed that SNs were identified in the mediastinum in 15 (35%) of 43 patients and the lymphatic route to each mediastinal lymph node station was lobe-specific.

GTS

TABLE 6. Patients who were converted to major lung resection

Patient No.	Age/sex	Histologic type	Planned segmentectomy	SN with metastasis	Converted procedure	Pathologic TNM
1	70/M	Ad	Apical segment of RLL	No. 13	Lobectomy	T1 N1 M0
2	72/M	Ad	Apical segment of RLL	No. 11	Lobectomy	T2 N1 M0
3	80/M	Ad	Posterior apical segment of LUL	No. 5	Upper division segmentectomy	T1 N2 M0

SN, Sentinel node; *Ad*, adenocarcinoma; *RLL*, right lower lobe; *LUL*, left upper lobe.

Therefore, to determine the intraoperative indication for segmentectomy without using SN identification, not only hilar lymph nodes but also lobe-specific mediastinal lymph nodes should be submitted for intraoperative frozen section diagnosis. The SN identification can target the lymph nodes among those.

The identification rate of SNs was 83% in the present study, as it was in the data of previous reports by several authors, that is, 63% to 82%.[12-14] We[14] previously reported the results of SN identification in 104 patients with clinical stage I NSCLC. Of the 104 patients, 15 patients had N1 or N2 disease. Although SN could be found to have metastases during the operation in 13 (87%) of those 15 patients, it produced false negative results in the remaining 2 patients. One of the 2 patients had T2 tumor and metastasis in the No. 12 nodal station, and the other had T1 tumor and metastasis in the No. 14 nodal station, which could not be identified as SN by our procedure because of its intrapulmonary location. We therefore believe that SN could be identified by our procedure in most of the patients with T1 N0 M0 NSCLC.

Although it has been reported that 20% to 25% of patients with clinical stage I disease have mediastinal lymph node metastasis,[22,23] the present study showed only 3 (6%) of 52 patients with N1 or N2 disease. Our procedure for lymph node dissection was systematic and then yielded 6 ± 1.8 nodal stations and 12.5 ± 6 lymph nodes to be dissected per patient. The low number of patients with N1 or N2 disease in the present study is probably due to the institutional setting; that is, most lung cancers in our patients were found by routine CT examination, resulting in a higher rate of early-stage NSCLC than usual.

The Lung Cancer Study Group study in 1995 (the only prospective randomized trial of lobectomy versus limited resection for T1 N0 NSCLC) reported that limited resection was inferior to lobectomy regarding death rate and local recurrence.[1] However, the study included a significant number (33%) of wedge resections in the limited resection group and did not analyze the results of segmentectomy. In addition, compared with clinical staging in 1995 when the Lung Cancer Study Group study was reported, it is now more accurate because of improved CT and FDG-PET technology. Therefore, a prospective randomized trial of lobectomy versus segmentectomy should be performed for c-T1 N0 M0 NSCLC. The SN navigation segmentectomy, which can target lymph nodes for intraoperative frozen section diagnosis, is a reasonable procedure for determining the final indication of segmentectomy.

GTS

References

1. Lung Cancer Study Group, Ginsberg RH, Rubinstein LV. Randomized trial of lobectomy versus limited resection for T1N0 non–small cell lung cancer. *Ann Thorac Surg.* 1995;60:615-23.
2. Jensik RJ, Faber LP, Milloy FJ, Monson DO. Segmental resection for lung carcinoma. *J Thorac Cardiovasc Surg.* 1973;66:563-72.
3. Tsubota N, Ayabe K, Doi O, Mori T, Namikawa S, Taki T, et al. Ongoing prospective study of segmentectomy for small lung tumors. *Ann Thorac Surg.* 1998;66:1787-90.
4. Okada M, Yoshikawa K, Hatta T, Tsubota N. Is segmentectomy with lymph node assessment an alternative to lobectomy for non–small cell lung cancer of 2 cm or smaller? *Ann Thorac Surg.* 2001;71:956-61.
5. Yoshikawa K, Tsubota N, Kodama K, Ayabe H, Taki T, Mori T. Prospective study of extended segmentectomy for small lung tumors: the final report. *Ann Thorac Surg.* 2002;73:1055-9.
6. Kodama K, Doi O, Higashiyama M, Yokouchi H. Intentional limited resection for selected patients with T1 N0 M0 non–small cell lung cancer. *J Thorac Cardiovasc Surg.* 1997;114:347-53.
7. Harada H, Okada M, Sakamoto T, Matsuoka H, Tsubota N. Functional advantage after radical segmentectomy versus lobectomy for lung cancer. *Ann Thorac Surg.* 2005;80:2041-5.
8. Warren WH, Faber LP. Segmentectomy versus lobectomy in patients with stage I pulmonary carcinoma: five-year survival and patterns of intrathoracic recurrence. *J Thorac Cardiovasc Surg.* 1994;107:1087-93.
9. Tafra L, Lannin DR, Swanson MS, Eyk JJV, Verbanac KM, Chua AN, et al. Multicenter trial of sentinel node biopsy for breast cancer using both technetium sulfur colloid and isosulfan blue dye. *Ann Surg.* 2001;233:51-9.
10. Morton DL, Thompson JF, Essner R, Elashoff R, Stern SL, Nieweg OE, et al. Validation of the accuracy of intraoperative lymphatic mapping and sentinel lymphadenectomy for early-stage melanoma. *Ann Surg.* 1999;230:453-65.
11. Kitagawa Y, Fujii H, Mukai M, Kubota T, Ando N, Watanage M, et al. The role of the sentinel lymph node in gastrointestinal cancer. *Surg Clin North Am.* 2000;80:1799-809.
12. Liptay MJ, Masters GA, Winchester DJ, Edelman BL, Carrido BJ, Hirshtritt TR, et al. Intraoperative radioisotope sentinel lymph node mapping in non-small cell lung cancer. *Ann Thorac Surg.* 2000;70:384-90.
13. Nomori H, Horio H, Naruke T, Orikasa H, Yamazaki K, Suemasu K. Use of technetium-99m tin colloid for sentinel lymph node identification in non–small cell lung cancer. *J Thorac Cardiovasc Surg.* 2002; 124:486-92.
14. Nomori H, Watanabe K, Ohtsuka T, Naruke T, Suemasu K. In vivo identification of sentinel lymph nodes for clinical stage I non–small cell lung cancer for abbreviation of mediastinal lymph node dissection. *Lung Cancer.* 2004;46:49-55.
15. Sobin LH, Wittekind CH, editors. UICC: TNM classification of malignant tumors. 6th ed. New York: John Wiley & Sons; 2002.

16. Naruke T, Suemasu K, Ishikawa S. Lymph node mapping and curability at various levels of metastasis in resected lung cancer. *J Thorac Cardiovasc Surg.* 1978;76:832-9.
17. Naruke T, Tsuchiya R, Kondo H, Nakayama H, Asamura H. Lymph node sampling in lung cancer: how should it be done? *Eur J Cardiothorac Surg.* 1999;16:S17-24.
18. Shimizu J, Oda M, Hayashi Y, Nonomura A, Watanabe Y. A clinicopathologic study of resected cases of adenosquamous carcinoma of the lung. *Chest.* 1996;109:9889-94.
19. Nakagawa K, Yasumitsu T, Fukuhara K, Shiono H, Kikui M. Poor prognosis after lung resection for patients with adenosquamous carcinoma of the lung. *Ann Thorac Surg.* 2003;75:1740-4.
20. Okada M, Tsubota N, Yoshimura M, Miyamoto Y, Matsuoka H. Prognosis of completely resected pN2 non–small cell lung carcinomas: what is the significant node that affects survival? *J Thorac Cardiovasc Surg.* 1999;118:270-5.
21. Riquet M, Hidden G, Debesse B. Direct lymphatic drainage of lung segments to the mediastinal nodes. *J Thorac Cardiovasc Surg.* 1989;97:623-32.
22. Seely JM, Mayo JR, Miller RR, Muller NL. T1 lung cancer: prevalence of mediastinal node metastases and diagnostic accuracy of CT. *Radiology.* 1993;186:129-32.
23. Heavey LR, Glazer GM, Gross BH, Francis IR, Orringer MB. The role of CT in staging radiographic T1N0M0 bronchogenic cancer. *AJR.* 1986;146:285-90.

GTS

03(XVIII)-99

5-Aminolevulinic Acid(5-ALA)を応用した術中脳腫瘍同定 －半導体レーザと光ファイバを用いた局所計測法－

○清水 一秀[1] 小林 英津子[1] 丸山 隆志[2] 村垣 善浩[2] 伊関 洋[2] 佐久間 一郎[1]

[1]東京大学大学院新領域創成科学研究科,

[2]東京女子医科大学大学院先端生命医科学研究所先端工学外科

Intraoperative detection of brain tumor using 5-Aminolevulinic Acid (5-ALA)

-study on point measurement with a laser diode and an optical fiber-

[1]K.Shimizu, [1]E.Kobayashi, [4]T.Maruyama, [4]Y.Muragaki, [4]H.Iseki and [1]I.Sakuma

[1]*Graduate School of Frontier Sciences, The University of Tokyo*

[2]*Faculty of Advanced Techno-Surgery, Institute of Advanced Biomedical Engineering and Science, Graduate School of Medicine, Tokyo Women's Medical University*

Abstract: In neurosurgery, tumor tissue must be removed as much as possible to prevent recurrence. We have studied on application of 5-Aminolevulinic Acid (5-ALA) as a tumor marker. 5-ALA biosynthetically induces a fluorescent substance called Protoporphyrin9 (Pp9). Pp9 is excited by blue or violet light and emits red fluorescence. Detection of the fluorescence can lead to precise removal of tumor. We introduced a blue-violet laser diode as an excitation light source and an optical fiber to collect the fluorescence. We aim to detect the fluorescence with high spatial resolution for better resection rate. To achieve this purpose, we focused the laser on the surface of brain tissue to limit the area to generate fluorescence. In this paper, we made an optical phantom for brain tumor taking scattering coefficient into account. And also, we studied on the effect of focusing laser beam changing laser spot diameter. Our result shows that broadening of illuminated area will increase the intensity of collected fluorescence. On the other hand, it may impair the spatial resolution. In addition, our new optical phantom is highly useful for 5-ALA study, especially for experiments for demarcation of tumor border.

Keywords: Neurosurgery, 5-ALA, 5-Aminolevulinic Acid, Protoporphyrin9, Point Measurement, Optical Phantom

1. はじめに

脳腫瘍の治療においては，腫瘍と正常組織の境界を術中に正確に判断する必要がある．5-Aminolevulinic Acid (5-ALA)は腫瘍細胞に選択的に取り込まれ，代謝を経て蛍光物質であるProtoporphyrin9 (Pp9)に変化する[1]．この蛍光を発する部位を同定することで腫瘍除去率の向上が期待される．すでに示した[2]ように，我々は蛍光同定方法の一つとして光ファイバによる局所計測を提案している．光源には半導体レーザ(LD)を採用した．キセノンランプなどを用いたこれまでの光源に比べ，限定的波長を持つLDは効率の良い励起が可能であり，同時に様々な応用可能性を持つ．我々はレーザの照射スポットを絞ることにより蛍光発生領域を制限し，蛍光検知における空間分解能の向上を試みた．レーザを広く照射するとその分広い領域から蛍光を集めることができるのでS/Nは向上するが，逆に空間分解能は損なわれると思われる．そこで，レーザの照射スポット径という観点から蛍光強度を考察した．また，生体組織は光に対し散乱が強いため，実験のために脳組織を模擬した光散乱特性をもつ生体模擬試料（ファントム）を製作し，検討した．

2. システム概要

蛍光誘導・検知システムの概要図をFig. 1に示す．我々のレーザ(406[nm],18[mW]，特注品，Digital Stream Corporation)は一定の焦点距離を持つように収束してのビーム照射が可能である．照射対象位置との距離を設定する事により照射スポット径を調節できる．蛍光はレーザを照射された部位から無指向的に放出されるものとし，レーザスポットの中心に向けてプラスチック光ファイバ(POF)を配置する．収集した光は光フィルタを通る事で蛍光のみが抽出され，フォトダイオードで蛍光強度の信号として検出される．ここで照射対象として用いたファントムは発光体であるPp9 の他に散乱物質としてイントラリピッド10%(IL)を加え，約1%のAgarを用いて均質なゲルとした．

3. 実験

(1) ファントムの製作

ILの濃度は参考文献[3], [4]から C=318[ml/l]と

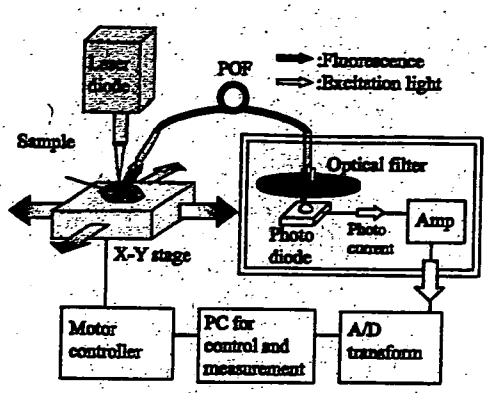

Fig.1 Overview of point measurement system.

した. Pp9 は 50[mg/l]とした. 比較対象として Pp9 を含まないファントムが必要であり, これらが明確な境界面を持つよう Fig.2 に示す容器を製作した. Agar によりファントムはゲル状なので境界面が保たれた.

(2) 蛍光強度測定

ファントムを X-Y ステージに載せ, レーザのパワーは約 2[mW]とし, 照射スポット径を 0.1, 0.5, 1.0, 1.5, 2.0, 2.5[mm]に設定した. それぞれについてスポット径の大きさによる影響を調べるため, すべてに共通な位置(Pp9 あり)においての蛍光強度を測定した. また, ファントム(Pp9 あり, なし)の境界線を垂直にまたぐように 20[mm]の距離を直線状にスキャンした. この測定は 5 回ずつ行い平均を算出した.

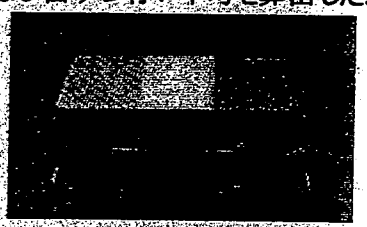

Fig.2 Optical phantom with two borders (one of them is mentioned in the paper)

4. 結果・考察

スポット径と蛍光強度の関係を Fig.3 に, 直線スキャンの結果を Fig.4 に示す. Fig.4 ではそれぞれのスポット径においてのスキャン方向の位置に対する蛍光強度が示されている. ここではファントムの境界面をと交差する部分を強調して示してある. Fig.3 より, スポット径が大きくなるにつれ, より広い領域から蛍光が放射されるので検出される蛍光強度は強くなると思われる. Fig.4 より, スポット径が小さいほど境界付近での蛍光強度の立ち上がりが急峻になった.

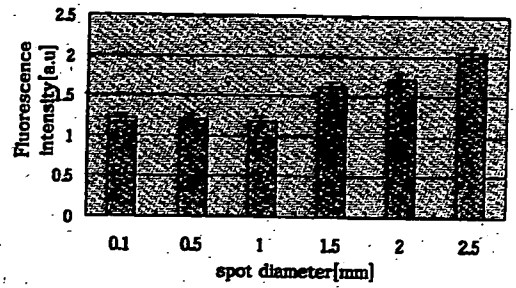

Fig.3 Fluorescence intensity versus spot diameter

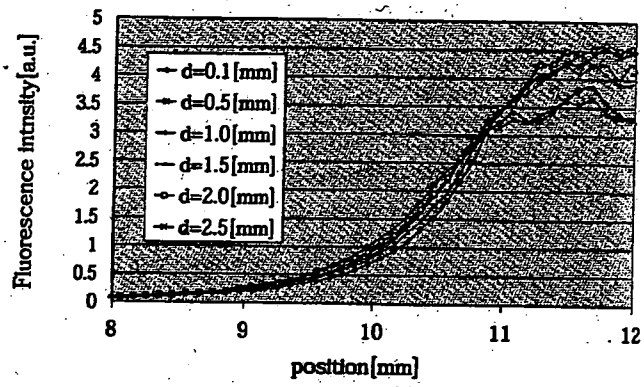

Fig.4 Fluorescence intensity versus position

5. 結論・展望

スポット径を広げることにより, 検出可能な蛍光強度が増すことが確認された. 分解能を規定するためには更なる検討が必要であるが, その際に今回製作した光学ファントムは非常に有用である.

文献

1) W. Stummer et al., Intraoperative Detection of Malignant Gliomas by 5-Aminolevulinic Acid-induced Porphyrin Fluorescence, Neurosurgery, vol.42, no.3, pp.518-526, 1998
2) K. Shimizu et al., Application of blue semiconductor laser to measurement of 5-ALA induced fluorescence for intraoperative detection of brain tumor, Proceedings of 6th Japan-France Congress on Mechatronics pp135-140, 2003
3) Hugo J. van Staveren et al., Light Scattering in Intralipid-10% in the wavelength range of 100-1100 nm, Applied Optics, vol.30, no.31, 1991
4) Vo-Dinh, Biomedical Photonics Handbook, CRC Press, 2003

04(III)-16

脳外科用レーザ手術装置のための小型オートフォーカスシステムの開発

○ 野口 雅史[a],青木 英祐[a],小林 英津子[a],大森 繁[b/c],村垣 善浩[c],伊関洋[c],佐久間 一郎[a]

[a]東京大学大学院新領域創成科学研究科,[b]テルモ(株)

[c]東京女子医科大学大学院先端生命医科学研究所先端工学外科

Development of a Compact Automatic Focusing System for a Neurosurgical Laser Instrument

M.Noguchi[a], E.Aoki[a], E.Kobayashi[a], S.Omori[b/c], Y.Muragaki[c], H.Iseki[c], I.Sakuma[a]

[a] *Graduate School of Frontier Sciences, The University of Tokyo,* [b] *Terumo Corporation*

[c] *Faculty of Advanced Techno-surgery, Institute of Biomedical Engineering and Science, Graduate School of Medicine, Tokyo Women's Medical University*

Abstract: In neurosurgery such as the treatment of glioma, it is very important to remove tumor as accurately as possible. A micro laser with wavelength of 2.8 [um] is suitable to remove the tumor on the brain surface because of its strong absorption feature by water. It is necessary, however, to keep the distance between the laser probe and the target at its focal length. We had developed an automatic-focusing system using a guide laser and a CCD camera and performed some experiments for evaluation *in vitro* and an *in vivo* test on a porcine brain. They showed that accuracy of focusing largely depends on the condition of the brain surface that is very noisy and fully abundant in scattering and absorption. In this research, we evaluated focusing accuracy by changing several parameters such as the wavelength of the guide laser and the value of the threshold for binarization. The results showed that it is necessary to control adequately and dynamically the threshold, the electronic shutter speed and the power of the guide laser to realize precise focusing on the brain surface.

Key words: Neurosurgery, Laser ablation, Automatic focusing, Medical robot, Brain tumor

1. はじめに

脳腫瘍の治療において，治療後の再発を防ぐために腫瘍と正常組織の境界部を精確に除去する外科的治療法が求められている．我々は，この脳腫瘍摘出後の残存部の除去法として，腫瘍細胞を波長2.8[μm]のマイクロレーザで蒸散させる方法を提案してきた[1]．このレーザは，レーザプローブの先端と対象物の距離を，ある一定範囲内に保たなければならない．そこで，我々はガイドレーザを用いてプローブ先端と対象面との距離を非接触で動的に測定し，プローブの位置補正を行うオートフォーカス機構の開発を行ってきた．これまで，試作機を製作し，追従性などの基本性能の評価，ブタを用いた *in vivo* での動作実験を行ってきた[2]．しかし、*In vivo* 実験において，血液による吸収が原因となり，ガイドレーザスポットの抽出が困難になる問題が生じた．生体組織において光は，散乱，吸収により減衰する．*In vivo* 実験においても，散乱，吸収特性によってスポットの抽出が困難となったといえる．

そこで本研究では，脳の各組織を模擬したファントムに対し、ガイドレーザ波長及び，スポット抽出のフィルタ条件に関する評価を行った．

2. フォーカシング方法

本システムでは，ガイドレーザと計測用小型 CCD カメラを用いた変位計測法によりフォーカスを行う．対象面に照射したガイドレーザのスポットをCCDカメラにより観察し，計測したスポット座標の変位を基にフォーカシングを行う．ガイドレーザには波長532[nm]のレーザダイオードを用いている．

スポットの座標は，CCDカメラにより得られたY(輝度)UV(色差)画像を輝度値に関して2値化を行い，スポットの抽出を行った後，重心座標を算出することにより決定している．

3. 実験方法と結果

3. 1レーザ波長及びフィルタ条件評価

各異なる組織に対して，ガイドレーザの波長，電子シャッター速度及び 2 値化の際の輝度閾値を変えスポットの計測を行い，各条件の評価を行った．

レーザの波長は 532[nm]と 635[nm]を選定した．